Noname manuscript No.
(will be inserted by the editor)

The optimised Schwarz method and the two-Lagrange multiplier method for heterogeneous problems in general domains with two general subdomains

Neil Greer · **Sébastien Loisel**

the date of receipt and acceptance should be inserted later

Abstract The optimised Schwarz method and the related two-Lagrange multiplier (2LM) method are nonoverlapping domain decomposition methods which can be used to numerically solve boundary value problems. Local Robin problems are solved on each subdomain in parallel to approximate the global solution, where a careful choice of Robin parameters leads to faster convergence. The 2LM method involves the solution of a nonsymmetric linear system that is usually solved with a Krylov subspace method such as GMRES. The speed of convergence of GMRES can be estimated using a conformal map from the exterior of the field of values of the system matrix to the interior of the unit disc. In this article we consider an elliptic PDE problem with a jump in diffusion coefficients across the interface between the subdomains. We approximate the field of values of the 2LM system matrix by a rectangle $\square$ in $\mathbb{C}$ and provide optimised Robin parameters that ensure that $\square$ is "well conditioned" in the sense that GMRES converges quickly. We derive convergence estimates for GMRES and consider the behaviour asymptotically as the mesh size h becomes small and the jump in coefficients becomes large. We observe, for our choice of Robin parameters, that increasing the jump in coefficients increases the convergence rate of GMRES. Numerical experiments are performed to verify the theoretical results.

Keywords Domain decomposition · Optimised Schwarz method · Two-Lagrange multiplier method · Heterogeneous media · GMRES convergence

N. Greer (✉)
Department of Mathematics, Heriot-Watt University, Edinburgh, EH14 4AS, United Kingdom
E-mail: dng30@hw.ac.uk

S. Loisel
E-mail: S.Loisel@hw.ac.uk

1 Introduction

Consider the model problem

$$\begin{cases} -\nabla \cdot (a(\boldsymbol{x})\nabla u) = f & \text{in} \quad \Omega \\ u = 0 & \text{on} \quad \partial\Omega. \end{cases} \tag{1.1}$$

The open set $\Omega \subset \mathbb{R}^n$ is partitioned into two nonoverlapping subdomains Ω_1, $\Omega_2 \subset \Omega$, such that

$$a(\boldsymbol{x}) = \begin{cases} \alpha_1 \alpha_0(\boldsymbol{x}) & \text{for} \quad \boldsymbol{x} \in \Omega_1 \\ \alpha_2 \alpha_0(\boldsymbol{x}) & \text{for} \quad \boldsymbol{x} \in \Omega_2, \end{cases}$$

where α_1, $\alpha_2 \in \mathbb{R}^+$ and $\alpha_0(\boldsymbol{x})$ is a continuous function with $0 < \alpha_{\min} < \alpha_0(\boldsymbol{x}) < \alpha_{\max} < \infty$. If $f \in L^2(\Omega)$, then the weak formulation of (1.1) has a solution $u \in H_0^1(\Omega)$.

Problems like (1.1) arise in physics and engineering and are usually solved numerically. After discretisation (e.g. using the piecewise linear finite element method) we obtain the linear system

$$A\boldsymbol{u} = \boldsymbol{f}, \tag{1.2}$$

where A is a large, sparse, symmetric positive definite matrix. Solving system (1.2) directly is impractical due to fill in so we use an iterative solver based on the domain decomposition methods (DDMs). These methods partition the physical domain into subdomains and solve smaller subdomain problems in parallel to construct a global solution.

We define the interface between the subdomains by

$$\Gamma = \Omega \cap (\partial\Omega_1 \cup \partial\Omega_2),$$

then $\Omega = \Omega_1 \cup \Omega_2 \cup \Gamma$. When $\alpha_1 \neq \alpha_2$ there is a discontinuity across Γ and (1.1) corresponds to a problem in heterogeneous media. Then the heterogeneity of the problem naturally defines a nonoverlapping decomposition of the physical domain Ω. Figure 1.1 shows an example of a nonoverlapping decomposition of a general domain.

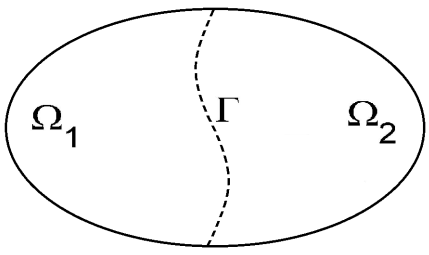

Fig. 1.1 nonoverlapping decomposition of a general domain into two general subdomains

The main idea behind DDMs and how the different methods arise is how to transfer information between the subdomains, by imposing suitable transmission conditions on Γ, such that the iterates applied to the subproblems piece together to give the global solution. We refer the reader to [21,23,27] for treatises on the subject of DDMs.

The earliest DDM, the classical Schwarz method, was introduced in [26] as a proof technique for the Riemann principle. The method imposes Dirichlet conditions on the interface between the subdomains but requires overlap to converge. In [17] Lions proposed a nonoverlapping variant of Schwarz's method that imposes Robin transmission conditions on Γ. Convergence was proved using energy estimates for any choice of Robin parameter $p > 0$. Optimised Schwarz methods (OSM), [11,13], aim to find optimal Robin parameters to speed up convergence. See [14] for a full history of the various Schwarz methods. Convergence of the OSM is usually proved using Fourier analysis, [10], and so the subdomains considered are restricted to being regular and rectangular. In [19] the author analyses the convergence for more general subdomains by considering the spectral radius of the interface operator that is expressed in terms of the Dirichlet to Neumann map (also known as the Poincaré-Steklov operator).

A DDM closely related to the OSM is the two-Lagrange multiplier (2LM) method introduced in [9]. The main idea behind the 2LM method is not to introduce an iteration explicitly but to replace the large linear system (1.2) with the smaller equivalent system

$$A_{2LM}\boldsymbol{\lambda} = \boldsymbol{c}, \tag{1.3}$$

where $\boldsymbol{\lambda}$ is a vector of Lagrange multipliers that are used to solve local Robin problems on the subdomains in parallel. Though we don't consider them in this paper the 2LM method is more suited than the OSM in dealing with cross points, which occur where three or more subdomains coincide. In [5,18] it was shown, for general subdomains with cross points, that if the Robin parameter on the interface is chosen to be of $O(h^{-1/2})$ the condition number of the 2LM method system matrix is of $O(h^{-1/2})$, where h is the finite element parameter. Efforts have been made, [12], to estimate the convergence of OSM in the presence of cross points. In the absence of cross points, when the subdomains are arranged in strips, it is known, [24], that the OSM and 2LM method are equivalent when a Richardson iteration is applied to system (1.3).

The results described thus far have been for problems in homogeneous media, i.e. there is no jump in coefficients between the subdomains. The OSM in heterogeneous media has been studied using Fourier analysis on rectangular subdomains in [6,20] and by estimating the spectral radius of the interface operator acting on general subdomains in [7]. Both approaches show that with a suitable choice of Robin parameters the speed of convergence of OSM is faster when the jump in coefficients becomes larger. In this article we propose to study the 2LM method for heterogeneous problems in a general domain with two general subdomains.

Even though system (1.2) may be symmetric the related 2LM method system (1.3) will be nonsymmetric. While smaller than the original system, it is still too costly to solve the 2LM system directly so we use an iterative Krylov subspace method for nonsymmetric systems such as GMRES (*Generalized Minimal RESidual*), [25]. The speed of convergence of GMRES can be estimated using a conformal

map from the exterior of the field of values of the system matrix to the interior of the unit disc, [3], where the field of values is a compact convex subset of $\mathbb{C}$ that contains the spectrum of a given matrix. A careful choice of Robin parameters will lead to a more favourable field of values of the 2LM system matrix and faster convergence of GMRES.

Our paper is organised as follows. In Section 2 we briefly outline the OSM and 2LM method for problems in heterogeneous media and show the equivalence between the two. In Section 3 we approximate the field of values of the 2LM method system matrix with a rectangle in $\mathbb{C}$. Our main results (Theorems 4.1, 4.2 and 4.3) are presented in Section 4, where we provide optimised Robin parameters and estimate the convergence rate of GMRES applied to the 2LM system (1.3). We study the asymptotic behaviour as the finite element parameter h becomes small and the jump between coefficients α_1 and α_2 becomes large, observing faster convergence as the jump is increased. In Section 5 we verify our results with some numerical experiments.

2 The optimised Schwarz method and the two-Lagrange multiplier method

2.1 The continuous optimised Schwarz method

Consider the model problem (1.1). For $i = 1, 2$, let a_i denote the restriction of coefficient $a(\boldsymbol{x})$ to subdomain Ω_i and u_i the restriction of the solution u to subdomain Ω_i. Then given initial guess u_i^0 the continuous form of the OSM iteration for $k = 1, 2, \ldots$ is: solve for $i = 1, 2$

$$\begin{cases} -a_i \Delta u_i^k = f & \text{in} \quad \Omega_i \\ u_i^k = 0 & \text{on} \quad \partial\Omega_i \cap \partial\Omega \\ (p_i + a_i \partial_{n_i}) u_i^k = (p_i + a_{3-i}\partial_{n_{3-i}}) u_{3-i}^{k-1} & \text{on} \quad \Gamma, \end{cases} \tag{2.1}$$

where ∂_{n_i} denotes the directional derivative with respect to the outward pointing normal n_i of $\partial\Omega_i$. Though in practice the Robin parameters $p_i \in (0, \infty)$ could vary along the interface here and throughout the paper we only consider the case where they are constant on Γ. A careful choice of these Robin parameters will speed up convergence considerably.

The version of the OSM we have presented above can be implemented in parallel, as system (2.1) can be solved simultaneously for each subdomain with the only exchange of information needed after each iteration to update the Robin relation in the third line. The difficulty arises in calculating the normal derivatives, however in [2] the author presents a formula for updating the Robin relation that avoids computing these derivatives. We next derive the discrete form of (2.1).

2.2 The discrete optimised Schwarz method

We assume the partition of the domain Ω into nonoverlapping subdomains, Ω_1 and Ω_2, is such that for both subdomains $\partial\Omega_i \cap \partial\Omega \neq \emptyset$, i.e. we have no subdomains that

"float". Suppose we perform a quasi-uniform triangulation of Ω, with mesh parameter h, into n degrees of freedom. The triangulation, $\mathscr{T}_h$, is such that each element lies in only one of the subdomains, so that the interface Γ does not "cut through" any elements. Once a suitable basis has been chosen for the finite element space $V_h \subset H_0^1(\Omega)$, we can construct the discretised form of (1.1) to obtain the linear system (1.2), with A an $n \times n$ sparse, symmetric positive definite matrix.

For each subdomain Ω_i we can define a restriction matrix R_i. If the triangulation $\mathscr{T}_h$ contains n_i degrees of freedom in subdomain Ω_i and n_Γ degrees of freedom on the interface Γ we let $m_i = n_i + n_\Gamma$. Then R_i is an $m_i \times n$ Boolean matrix that restricts an arbitrary n dimensional vector $\boldsymbol{u}$ to an m_i dimensional vector $R_i\boldsymbol{u}$ which contains only the entries of $\boldsymbol{u}$ corresponding to degrees of freedom in $\Omega_i \cup \Gamma$. The corresponding extension matrix R_i^T prolongs an arbitrary m_i dimensional vector to an n dimensional vector.

Using these restriction and extension matrices we can recover the global stiffness matrix and load vector from (1.2) through the relation

$$A = \sum_{i=1}^{2} \alpha_i R_i^T A_{N_i} R_i \qquad \text{and} \qquad \boldsymbol{f} = \sum_{i=1}^{2} R_i^T \boldsymbol{f}_i. \tag{2.2}$$

Here A_{N_i} are local stiffness matrices for the subdomains with entries given by

$$(A_{N_i})_{jk} = \int_{\Omega_i} \alpha_0(\boldsymbol{x}) \left(\nabla \phi_j \cdot \nabla \phi_k\right),$$

where $\phi_1, \ldots, \phi_k$ are the basis functions of the finite element space V_h. These matrices correspond to the discretisation of the Laplacian on subdomain Ω_i with Dirichlet boundary conditions on $\partial\Omega_i \setminus \Gamma$ and Neumann boundary conditions on Γ. The entries of $\boldsymbol{f}_i$ are given by $\int_{\Omega_i} f\phi_i$.

To take into account the Robin transmission conditions in (2.1) we next define the mass matrix M on the interface Γ with entries given by

$$(M)_{jk} = \int_\Gamma \phi_j \phi_k.$$

To simplify the implementation of the OSM it is judicious to lump this mass matrix. Then we replace M with the spectrally equivalent matrix hI, where h is the finite element mesh parameter and I the $n_\Gamma \times n_\Gamma$ identity matrix corresponding to the n_Γ degrees of freedom on Γ.

Now let $\boldsymbol{u}_i$ denote the restriction of the solution vector $\boldsymbol{u}$ to subdomain Ω_i. Then given initial guess $\boldsymbol{u}_i^0$ the discrete version of the optimised Schwarz method is for $k = 1, 2, \ldots$: solve for $i = 1, 2$

$$\begin{aligned}\Big(\alpha_i A_{N_i} + p_i B_i\Big)\boldsymbol{u}_i^k = R_i\Big(\boldsymbol{f} - \alpha_{3-i}\tilde{A}R_{3-i}^T\boldsymbol{u}_{3-i}^{k-1}\Big) \\ + \Big(\alpha_{3-i}A_{N_i} + p_i B_i\Big)R_i R_{3-i}^T \boldsymbol{u}_{3-i}^{k-1},\end{aligned} \tag{2.3}$$

where B_i is a matrix with entries equal to zero corresponding to vertices interior to Ω_i and entries equal to the lumped mass matrix corresponding to vertices on Γ. The matrix $\tilde{A}$ is the global stiffness matrix without the contribution of the diffusion coefficients, i.e. $\tilde{A} = \sum_{i=1}^{2} R_i^T A_{N_i} R_i$.

2.3 The two-Lagrange multiplier method

The 2LM method is closely related to the OSM but does does not directly introduce an iteration for system (1.2), rather a smaller equivalent system is solved. We consider the local Robin problems, for $i = 1, 2$

$$\begin{cases} -a_i \Delta u_i = f & \text{in} \quad \Omega_i \\ u_i = 0 & \text{on} \quad \partial\Omega_i \cap \partial\Omega \\ (p_i + a_i \partial_{n_i}) u_i = \lambda_i & \text{on} \quad \Gamma, \end{cases} \tag{2.4}$$

where the transmission conditions from subdomain Ω_{3-i} have been absorbed into the "Robin data" λ_i.

Following the formulation as presented in [27], we can write the local stiffness matrix A_{N_i} and load vector $\boldsymbol{f}_i$ in block form as

$$A_{N_i} = \begin{bmatrix} A_{II_i} & A_{I\Gamma_i} \\ A_{\Gamma I_i} & A_{\Gamma\Gamma_i} \end{bmatrix} \qquad \text{and} \qquad \boldsymbol{f}_i = \begin{bmatrix} \boldsymbol{f}_{I_i} \\ \boldsymbol{f}_{\Gamma_i} \end{bmatrix}.$$

Here the degrees of freedom have been partitioned into those internal to Ω_i and those on Γ. We can similarly partition the local solution vector into interior and interface blocks as $\boldsymbol{u}_i = [\boldsymbol{u}_{I_i}, \boldsymbol{u}_{\Gamma_i}]^T$. Then given a suitable "Robin data" vector $\boldsymbol{\lambda}_i$, the discrete form of (2.4) is given by

$$\begin{bmatrix} \alpha_i A_{II_i} & \alpha_i A_{I\Gamma_i} \\ \alpha_i A_{\Gamma I_i} & \alpha_i A_{\Gamma\Gamma_i} + p_i h I \end{bmatrix} \begin{bmatrix} \boldsymbol{u}_{I_i} \\ \boldsymbol{u}_{\Gamma_i} \end{bmatrix} = \begin{bmatrix} \boldsymbol{f}_{I_i} \\ \boldsymbol{f}_{\Gamma_i} \end{bmatrix} + \begin{bmatrix} 0 \\ \boldsymbol{\lambda}_i \end{bmatrix}, \tag{2.5}$$

where again the mass matrix has been lumped. We eliminate the interior nodes of (2.5) to obtain

$$(\alpha_i S_i + p_i h I)\, \boldsymbol{u}_{\Gamma_i} = \boldsymbol{g}_i + \boldsymbol{\lambda}_i, \tag{2.6}$$

where

$$S_i = A_{\Gamma\Gamma_i} - A_{\Gamma I_i} A_{II_i}^{-1} A_{I\Gamma_i} \quad \text{and} \quad \boldsymbol{g}_i = \boldsymbol{f}_{\Gamma_i} - A_{\Gamma I_i} A_{II_i}^{-1} \boldsymbol{f}_{I_i},$$

are the *Schur complement* of the Neumann matrix A_{N_i} and the *condensed right hand side* of the load vector $\boldsymbol{f}_i$ respectively. The Schur complement is the discrete form of the Dirichlet to Neumann map and since A_{N_i} is symmetric positive definite the corresponding S_i matrix is symmetric positive definite. The assumption that neither subdomain "floats" ensures that the Schur complement matrices are nonsingular.

Letting $p_s = \frac{(p_1+p_2)h}{2}$, (2.6) gives the relation

$$p_s \overbrace{\begin{bmatrix} \boldsymbol{u}_{\Gamma_1} \\ \boldsymbol{u}_{\Gamma_2} \end{bmatrix}}^{\boldsymbol{u}_G} = \overbrace{\begin{bmatrix} p_s(\alpha_1 S_1 + p_1 h I)^{-1} & 0 \\ 0 & p_s(\alpha_2 S_2 + p_2 h I)^{-1} \end{bmatrix}}^{Q} \left(\overbrace{\begin{bmatrix} \boldsymbol{g}_1 \\ \boldsymbol{g}_2 \end{bmatrix}}^{\boldsymbol{g}} + \overbrace{\begin{bmatrix} \boldsymbol{\lambda}_1 \\ \boldsymbol{\lambda}_2 \end{bmatrix}}^{\boldsymbol{\lambda}} \right). \tag{2.7}$$

Since we have two subdomains, the *many sided trace* $\boldsymbol{u}_G$ has pairs of entries for each degree of freedom on Γ and in general will correspond to a discontinuous function across Γ. For $\boldsymbol{u}_G$ to correspond to a continuous function the pairs of entries for each

node on Γ must all agree. To make this more precise consider the orthogonal projection matrix

$$K = \frac{1}{2}\begin{bmatrix} I & I \\ I & I \end{bmatrix},$$

where I is the $n_\Gamma \times n_\Gamma$ identity matrix, if n_Γ is the number of vertices on Γ. Matrix K acts to average function values for each degree of freedom on Γ and hence $\boldsymbol{u}_G$ corresponds to a continuous function across Γ when it satisfies the continuity condition:

$$K\boldsymbol{u}_G = \boldsymbol{u}_G \tag{2.8}$$

and the corresponding local solutions, $\boldsymbol{u}_i$, of (2.5) will meet continuously across Γ.

The 2LM method for (1.2) is to solve system (1.3) for $\boldsymbol{\lambda}$ where

$$A_{2LM} = (I-2K)(Q-K) \quad \text{and} \quad \boldsymbol{c} = -(I-2K)Q\boldsymbol{g}, \tag{2.9}$$

Vector $\boldsymbol{\lambda}$ is a many sided trace of Lagrange multipliers from which the method derives its name, as there are pairs of entries for each vertex on Γ. On solving (1.3) we have "Robin data" vectors $\boldsymbol{\lambda}_i$ that are plugged into the local problems (2.5), which can then be solved in parallel. The resulting local solutions $\boldsymbol{u}_i$ meet continuously across Γ and will "glue together" in a suitable way to give the global solution $\boldsymbol{u}$ of (1.2) such that $\boldsymbol{u}_i = R_i\boldsymbol{u}$.

Lemma 2.1 *Problem (1.3) is equivalent to (1.2).*

Proof To recover the solution, $\boldsymbol{u}$, of (1.2) from that of (1.3), the "Robin data" vectors $\boldsymbol{\lambda}_1$ and $\boldsymbol{\lambda}_2$ must solve the local Robin problems (2.5), such that the local solutions $\boldsymbol{u}_1$ and $\boldsymbol{u}_2$ meet continuously across the interface Γ. So first we check that continuity condition (2.8) holds. From (1.3) and (2.9) we have that

$$\begin{aligned} \boldsymbol{\lambda} &= -(Q-K)^{-1}(I-2K)^{-1}(I-2K)Q\boldsymbol{g} \\ &= -(Q-K)^{-1}Q\boldsymbol{g}. \end{aligned} \tag{2.10}$$

The above together with (2.7) gives us

$$\begin{aligned} \boldsymbol{u}_G &= \frac{1}{p_s}Q(\boldsymbol{g}+\boldsymbol{\lambda}) \\ &= \frac{1}{p_s}Q(\boldsymbol{g}-(Q-K)^{-1}Q\boldsymbol{g}) \\ &= \frac{1}{p_s}((Q-K)-Q)(Q-K)^{-1}Q\boldsymbol{g} \\ &= -\frac{1}{p_s}K(Q-K)^{-1}Q\boldsymbol{g}. \end{aligned}$$

Then since K is an orthogonal projection matrix:

$$\begin{aligned} K\boldsymbol{u}_G &= -\frac{1}{p_s}K^2(Q-K)^{-1}Q\boldsymbol{g} \\ &= -\frac{1}{p_s}K(Q-K)^{-1}Q\boldsymbol{g}. \end{aligned}$$

Hence $K\boldsymbol{u}_G = \boldsymbol{u}_G$ as required.

Imposing continuity across the interface is not sufficient, we must also ensure that the "fluxes" match as well. By the continuity condition there exists a unique $\boldsymbol{u}$ that restricts to $\boldsymbol{u}_i$:

$$\boldsymbol{u}_i = R_i\boldsymbol{u} \qquad \text{for } i = 1, 2. \tag{2.11}$$

If we impose on the solution $\boldsymbol{u}$ that equation (1.2) holds we obtain

$$\begin{aligned}
\boldsymbol{f} = A\boldsymbol{u} &= \sum_{i=1}^{2} \alpha_i R_i^T A_{N_i} R_i \boldsymbol{u} && \text{(using (2.2))} \\
&= \sum_{i=1}^{2} \alpha_i R_i^T A_{N_i} \boldsymbol{u}_i && \text{(using (2.11))} \\
&= \boldsymbol{f} + \sum_{i=1}^{2} R_i^T \begin{bmatrix} 0 \\ \boldsymbol{\lambda}_i - p_i h \boldsymbol{u}_{\Gamma_i} \end{bmatrix}. && \text{(using (2.2) and (2.5))}
\end{aligned}$$

Cancelling the $\boldsymbol{f}$ terms on each side, for the "fluxes" to match across the interface we need

$$\sum_{i=1}^{2} \boldsymbol{\lambda}_i - p_i h \boldsymbol{u}_{\Gamma_i} = 0. \tag{2.12}$$

As continuity condition (2.8) holds we have that $\boldsymbol{u}_{\Gamma_1} = \boldsymbol{u}_{\Gamma_2}$ and so $\boldsymbol{u}_G = [\boldsymbol{u}_{\Gamma_1}, \boldsymbol{u}_{\Gamma_1}]^T$. Then the left hand side of (2.12) becomes

$$\begin{aligned}
[I \quad I](\boldsymbol{\lambda} - p_s \boldsymbol{u}_G) &= [I \quad I](\boldsymbol{\lambda} - Q(\boldsymbol{g} + \boldsymbol{\lambda})) && \text{(using (2.7))} \\
&= [I \quad I]((K + (I-K) - Q)\boldsymbol{\lambda} - Q\boldsymbol{g}) \\
&= [I \quad I](-(Q-K)\boldsymbol{\lambda} - Q\boldsymbol{g} + (I-K)\boldsymbol{\lambda}) \\
&= [I \quad I](Q\boldsymbol{g} - Q\boldsymbol{g} + (I-K)\boldsymbol{\lambda}) && \text{(using (2.10))} \\
&= 0,
\end{aligned}$$

as required.

□

We next show the equivalence between the OSM and the 2LM method in the absence of cross points when system (1.3) is solved using a Richardson iteration.

Lemma 2.2 *Let $\boldsymbol{\lambda}_i^k$ be generated by a Richardson iteration applied to (1.3):*

$$\boldsymbol{\lambda}^k = \boldsymbol{\lambda}^{k-1} + 2(\boldsymbol{c} - A_{2LM}\boldsymbol{\lambda}^{k-1}). \tag{2.13}$$

Let $\boldsymbol{u}_i^k$ be generated by the OSM iteration (2.3). Assume that $\boldsymbol{u}_i^k$ solves

$$\begin{bmatrix} \alpha_i A_{II_i} & \alpha_i A_{I\Gamma_i} \\ \alpha_i A_{\Gamma I_i} & \alpha_i A_{\Gamma\Gamma_i} + p_i h I \end{bmatrix} \begin{bmatrix} \boldsymbol{u}_{I_i}^k \\ \boldsymbol{u}_{\Gamma_i}^k \end{bmatrix} = \begin{bmatrix} \boldsymbol{f}_{I_i} \\ \boldsymbol{f}_{\Gamma_i} + \boldsymbol{\lambda}_i^k \end{bmatrix}, \tag{2.14}$$

when $k = 0$. Then $\boldsymbol{u}_i^k$ solves (2.14) for all k.

Proof First consider the iterates produced by (2.13):

$$\boldsymbol{\lambda}_i^k = 2p_s(\alpha_{3-i}S_{3-i}+p_{3-i}hI)^{-1}\boldsymbol{g}_{3-i}+(2p_s(\alpha_{3-i}S_{3-i}+p_{3-i}hI)^{-1}-I)\boldsymbol{\lambda}_{3-i}^{k-1}, \quad (2.15)$$

for $i = 1,2$. Now consider the local Robin problem

$$\begin{bmatrix} \alpha_{3-i}A_{II_{3-i}} & \alpha_{3-i}A_{I\Gamma_{3-i}} \\ \alpha_{3-i}A_{\Gamma I_{3-i}} & \alpha_{3-i}A_{\Gamma\Gamma_{3-i}}+p_{3-i}hI \end{bmatrix} \begin{bmatrix} \tilde{\boldsymbol{u}}_{I_{3-i}}^k \\ \tilde{\boldsymbol{u}}_{\Gamma_{3-i}}^k \end{bmatrix} = \begin{bmatrix} \boldsymbol{f}_{I_{3-i}} \\ \boldsymbol{f}_{\Gamma_{3-i}}+\boldsymbol{\lambda}_{3-i}^k \end{bmatrix}.$$

Eliminating the interior nodes and rearranging we have

$$\boldsymbol{\lambda}_{3-i}^k = (\alpha_{3-i}S_{3-i}+p_{3-i}hI)\tilde{\boldsymbol{u}}_{\Gamma_{3-i}}^k - \boldsymbol{g}_{3-i}. \quad (2.16)$$

Recall that $p_s = \frac{p_i+p_{3-i}}{2}h$. Then plugging (2.16) into (2.15) gives

$$\begin{aligned} \boldsymbol{\lambda}_i^k &= (p_i+p_{3-i})h\tilde{\boldsymbol{u}}_{3-i}^{k-1} - (\alpha_{3-i}S_{3-i}+p_{3-i}hI)\tilde{\boldsymbol{u}}_{\Gamma_{3-i}}^{k-1}+\boldsymbol{g}_{3-i} \\ &= -(\alpha_{3-i}S_{3-i}-p_ihI)\tilde{\boldsymbol{u}}_{\Gamma_{3-i}}^{k-1}+\boldsymbol{g}_{3-i}. \end{aligned} \quad (2.17)$$

Combining (2.16) and (2.17) we obtain the iteration:

$$(\alpha_iS_i+p_ihI)\tilde{\boldsymbol{u}}_{\Gamma_i}^k - \boldsymbol{g}_i = -(\alpha_{3-i}S_{3-i}-p_ihI)\tilde{\boldsymbol{u}}_{\Gamma_{3-i}}^{k-1}+\boldsymbol{g}_{3-i}. \quad (2.18)$$

Now consider the OSM iteration, (2.3), which on eliminating the interior nodes gives

$$(\alpha_iS_i+p_ihI)\boldsymbol{u}_{\Gamma_i}^k = \boldsymbol{g}_i+\boldsymbol{f}_{I_{3-i}} - (\alpha_{3-i}A_{\Gamma\Gamma_{3-i}}-p_ihI)\boldsymbol{u}_{\Gamma_{3-i}}^{k-1} - \alpha_{3-i}A_{\Gamma I_{3-i}}\boldsymbol{u}_{I_{3-i}}^{k-1}. \quad (2.19)$$

We have from (2.14) that

$$\boldsymbol{u}_{I_{3-i}}^k = \frac{1}{\alpha_{3-i}}A_{II_{3-i}}^{-1}(\boldsymbol{f}_{I_{3-i}} - \alpha_{3-i}A_{I\Gamma_{3-i}}\boldsymbol{u}_{\Gamma_{3-i}}^k),$$

which substituting into (2.19) and rearranging gives the iteration:

$$(\alpha_iS_i+p_ihI)\boldsymbol{u}_{\Gamma_i}^k - \boldsymbol{g}_i = -(\alpha_{3-i}S_{3-i}-p_ihI)\boldsymbol{u}_{\Gamma_{3-i}}^{k-1}+\boldsymbol{g}_{3-i}. \quad (2.20)$$

Then provided iterations (2.18) and (2.20) have the same initial guess, that is $\tilde{\boldsymbol{u}}_{\Gamma_i}^0 = \boldsymbol{u}_{\Gamma_i}^0$, they will produce the same iterates.

□

Although iteration (2.13) will converge, it is faster to solve system (1.3) with a Krylov subspace method. Since the matrix A_{2LM} is nonsymmetric we need to use a method such as GMRES whose speed of convergence we are interested in.

3 The field of values of the 2LM method system matrix

3.1 The field of values and the convergence of GMRES

For an arbitrary matrix $A \in \mathbb{C}^{n\times n}$ the *field of values* (also known as the numerical range) of A is the compact convex subset of $\mathbb{C}$ defined by

$$W(A) = \{\boldsymbol{w}^* A\boldsymbol{w} : \boldsymbol{w} \in \mathbb{C}^n, \boldsymbol{w}^*\boldsymbol{w} = 1\}.$$

In particular $W(A)$ is the set of all Rayleigh quotients and hence contains the spectrum of A. If A is normal $W(A)$ is the convex hull of the set of eigenvalues of A, while if A is Hermitian $W(A)$ is an interval on the real line with endpoints given by the smallest and largest eigenvalues of A.

The *numerical radius* of A is a norm given by $r(A) = \max\{|z| : z \in W(A)\}$, equivalent to the 2-matrix norm $|||\cdot|||_2$ through the relation $|||A|||_2 \leq 2r(A) \leq 2|||A|||_2$. For full details of the field of values and the numerical radius see [15]. We next show the relationship between $W(A)$ and the convergence speed of GMRES.

For a given linear system $A\boldsymbol{x} = \boldsymbol{b}$, A not necessarily symmetric, and initial guess $\boldsymbol{x}_0$ the GMRES algorithm at iteration k generates an approximate solution $\boldsymbol{x}_k$ by automatically finding a polynomial $p_k(z)$ that satisfies the minimal residual property

$$\|\boldsymbol{r}_k\|_2 = \min_{\substack{p_k\in\mathscr{P}_k \\ p_k(0)=1}} \|p_k(A)\boldsymbol{r}_0\|_2. \tag{3.1}$$

Here $\boldsymbol{r}_k = \boldsymbol{b} - A\boldsymbol{x}_k$ is the residual at step k and $\mathscr{P}_k$ the set of all polynomials of degree $\leq k$. A typical convergence criterion of GMRES is to stop the iteration if $\|\boldsymbol{r}_k\|_2/\|\boldsymbol{r}_0\|_2$ reaches a given tolerance. Using the field of values $W(A)$ we can approximate how fast this quotient decreases towards zero.

If $W(A)$ does not contain the origin it is known, [8], that

$$r(p_k(A)) \leq \max_{z\in W(A)} |p_k(z)|,$$

then, using the fact that $|||p_k(A)|||_2 \leq 2r(p_k(A))$, (3.1) gives us

$$\frac{\|\boldsymbol{r}_k\|_2}{\|\boldsymbol{r}_0\|_2} \leq 2\overbrace{\min_{\substack{p_k\in\mathscr{P}_k \\ p_k(0)=1}} \max_{z\in W(A)} |p_k(z)|}^{E_k}.$$

The *estimated asymptotic convergence factor* is defined by

$$\rho = \lim_{k\to\infty} (E_k)^{1/k},$$

where $\rho \leq 1$, and an estimate for the convergence speed of GMRES is given by

$$\frac{\|\boldsymbol{r}_k\|_2}{\|\boldsymbol{r}_0\|_2} \approx 2\rho^k.$$

Since $W(A)$ is a connected set in $\mathbb{C}$ a formula for ρ can be derived through the use of conformal mappings, [3]. Let $\Phi(z)$ denote the conformal map from the exterior

of $W(A)$ to the interior of the unit disc with $\Phi(\infty) = 0$. Such a map exists by the Riemann mapping theorem, since the exterior of $W(A)$ is simply connected in the extended complex plane $\mathbb{C} \cup \{\infty\}$. Then provided $0 \notin W(A)$ the estimated asymptotic convergence factor is given by

$$\rho = |\Phi(0)|. \tag{3.2}$$

For the full derivation of (3.2) see [22].

In particular, the above formula for ρ will hold for any $\Phi(z)$ that is the conformal map from the exterior of a connected set, which contains the spectrum of the system matrix but does not contain the origin. Then by approximating $W(A_{2LM})$ by a connected set in $\mathbb{C}$ we can estimate the convergence speed of GMRES when solving (1.3).

3.2 Approximation of the field of values of the 2LM method system matrix by a rectangle

A simple numerical algorithm due to Johnson, [16], can be used to approximate the field of values of a matrix $A \in \mathbb{C}^{n\times n}$. It uses the property that any matrix can be split into Hermitian and skew-Hermitian parts. Let $H(A) = \frac{1}{2}(A + A^*)$ denote the Hermitian part of matrix A while $\sigma_{\min}(B)$ and $\sigma_{\max}(B)$ denote the smallest and largest eigenvalues of a Hermitian matrix B respectively. Now, using the fact that the field of values of a Hermitian matrix is an interval on the real line, we have that

$$\min_{z\in W(A)} \Re e(z) = \min_{\gamma\in W(H(A))} \gamma = \sigma_{\min}(H(A))$$

and

$$\max_{z\in W(A)} \Re e(z) = \max_{\gamma\in W(H(A))} \gamma = \sigma_{\max}(H(A)).$$

Then $W(A)$ lies in between the lines that run parallel to the imaginary axis, cross the real axis at points $\sigma_{\min}(H(A))$ and $\sigma_{\max}(H(A))$ and which intersect $W(A)$ on its boundary. Now, using the property that $W(e^{i\varphi}A) = e^{i\varphi}W(A)$, we can calculate $\sigma_{\min}(H(e^{i\varphi}A))$ and $\sigma_{\max}(H(e^{i\varphi}A))$ for different angles φ to find boundary points of $W(A)$. If A is real $W(A)$ is symmetric with respect to the real axis and we need only take $\varphi \in [0, \pi/2]$. Using this approach we can approximate the field of values of the 2LM method system matrix by a rectangle in $\mathbb{C}$. We first give a result for general matrices that have a special block structure.

Lemma 3.1 *Let X and Y be real, symmetric matrices of the same size and let $\tau \in \mathbb{R}$. Consider matrix A of the form:*

$$A = \begin{bmatrix} \tau I & X \\ Y & \tau I \end{bmatrix}.$$

Then $W(A)$ is contained in a rectangle in $\mathbb{C}$ centred at the point $(\tau, 0)$ with sides parallel to the imaginary axis defined by the lines $\{\tau \pm \frac{1}{2}\rho(X+Y) + \xi i : \xi \in \mathbb{R}\}$ and top and base parallel to the real axis defined by the lines $\{\pm\frac{1}{2}\rho(X-Y)i + \xi : \xi \in \mathbb{R}\}$. Where $\rho(\cdot)$ denotes the spectral radius of a symmetric matrix.

Proof For $\varphi \in [0, \pi/2]$ we have that

$$H(e^{i\varphi}A) = \frac{e^{i\varphi}}{2}\begin{bmatrix}\tau I & X\\ Y & \tau I\end{bmatrix} + \frac{e^{-i\varphi}}{2}\begin{bmatrix}\tau I & Y\\ X & \tau I\end{bmatrix}$$
$$= \begin{bmatrix}\tau\cos\varphi I & \frac{1}{2}(e^{i\varphi}X + e^{-i\varphi}Y)\\ \frac{1}{2}(e^{i\varphi}Y + e^{-i\varphi}X) & \tau\cos\varphi I\end{bmatrix}.$$

Say that A is $n \times n$, let $\boldsymbol{w} \in \mathbb{C}^n$ be such that $\boldsymbol{w}^*\boldsymbol{w} = 1$ and partition $\boldsymbol{w}$ into block form:

$$\boldsymbol{w} = \begin{bmatrix}\boldsymbol{u}\\ \boldsymbol{v}\end{bmatrix},$$

and so $\boldsymbol{u}^*\boldsymbol{u} + \boldsymbol{v}^*\boldsymbol{v} = 1$. Let $z_\varphi = \boldsymbol{w}^*H(e^{i\varphi}A)\boldsymbol{w}$, then $\{e^{-i\varphi}(z_\varphi + \xi i) : \xi \in \mathbb{R}\}$ defines a supporting hyperplane for $W(A)$, where

$$z_\varphi = \begin{bmatrix}\boldsymbol{u}^* & \boldsymbol{v}^*\end{bmatrix}\begin{bmatrix}\tau\cos\varphi I & \frac{1}{2}(e^{i\varphi}X + e^{-i\varphi}Y)\\ \frac{1}{2}(e^{i\varphi}Y + e^{-i\varphi}X) & \tau\cos\varphi I\end{bmatrix}\begin{bmatrix}\boldsymbol{u}\\ \boldsymbol{v}\end{bmatrix}$$
$$= \tau\cos\varphi + \frac{1}{2}\boldsymbol{u}^*\left(e^{i\varphi}X + e^{-i\varphi}Y\right)\boldsymbol{v} + \frac{1}{2}\boldsymbol{v}^*\left(e^{i\varphi}Y + e^{-i\varphi}X\right)\boldsymbol{u}.$$

Taking the absolute value and using Young's inequality, $ab \le \frac{a^2}{2} + \frac{b^2}{2}$, gives

$$\begin{aligned}\left|z_\varphi - \tau\cos\varphi\right| &\le \frac{1}{2}\left|\boldsymbol{u}^*(e^{i\varphi}X + e^{-i\varphi}Y)\boldsymbol{v}\right| + \frac{1}{2}\left|\boldsymbol{v}^*(e^{i\varphi}Y + e^{-i\varphi}X)\boldsymbol{u}\right|\\ &\le \frac{1}{2}||\boldsymbol{u}||_2||\boldsymbol{v}||_2\left(\left|\left|\left|e^{i\varphi}X + e^{-i\varphi}Y\right|\right|\right|_2 + \left|\left|\left|e^{i\varphi}Y + e^{-i\varphi}X\right|\right|\right|_2\right)\\ &\le \frac{1}{2}\left(\frac{||\boldsymbol{u}||_2^2}{2} + \frac{||\boldsymbol{v}||_2^2}{2}\right)\left(\left|\left|\left|e^{i\varphi}X + e^{-i\varphi}Y\right|\right|\right|_2 + \left|\left|\left|e^{i\varphi}Y + e^{-i\varphi}X\right|\right|\right|_2\right)\\ &= \frac{1}{4}\left(\left|\left|\left|e^{i\varphi}X + e^{-i\varphi}Y\right|\right|\right|_2 + \left|\left|\left|e^{i\varphi}Y + e^{-i\varphi}X\right|\right|\right|_2\right). \qquad (3.3)\end{aligned}$$

These matrix norms are in general difficult to estimate, but we have two special values of φ that simplify bound (3.3). When $\varphi = 0$:

$$|z_0 - \tau| \le \frac{1}{4}|||X + Y|||_2 + \frac{1}{4}|||Y + X|||_2$$
$$= \frac{1}{2}\rho(X + Y), \qquad (3.4)$$

where we have used the fact that $|||A|||_2 = \rho(A)$, if A is symmetric. While for $\varphi = \pi/2$:

$$\left|z_{\frac{\pi}{2}}\right| \le \frac{1}{4}|||iX - iY|||_2 + \frac{1}{4}|||iY - iX|||_2$$
$$= \frac{1}{2}\rho(X - Y). \qquad (3.5)$$

Then the lines that run through the points defined by (3.4) and (3.5) form a rectangle in $\mathbb{C}$ centred at the point $(\tau,0)$, with top and bottom parallel to the real axis and sides parallel to the imaginary axis, that contains $W(A)$.

□

Corollary 3.1 *Let* $X = 1 - p_s(\alpha_2 S_2 + p_2 hI)^{-1}$, $Y = 1 - p_s(\alpha_1 S_1 + p_1 hI)^{-1}$ *and* $\tau = 1/2$. *The 2LM method system matrix is of the form:*

$$A_{2LM} = \begin{bmatrix} \frac{1}{2}I & X \\ Y & \frac{1}{2}I \end{bmatrix}.$$

Then $W(A_{2LM})$ *is contained in the rectangle,* $\square$, *centred at the point* $(1/2,0)$ *with sides defined by the lines* $\{\frac{1}{2} \pm \frac{1}{2}\mathscr{R}(p_1,p_2) + \xi i : \xi \in \mathbb{R}\}$ *and top and base defined by the lines* $\{\pm\frac{1}{2}\mathscr{I}(p_1,p_2)i + \xi : \xi \in \mathbb{R}\}$, *with*

$$\mathscr{R}(p_1,p_2) = \max\{|\mu_1(p_1,p_2)|, |\mu_2(p_1,p_2)|\},$$

where

$$\mu_1(p_1,p_2) = 1 - p_s\left(\frac{1}{\alpha_1 s_{\min} + p_1 h} + \frac{1}{C_1\alpha_2 s_{\min} + p_2 h}\right)$$

and

$$\mu_2(p_1,p_2) = 1 - p_s\left(\frac{1}{\alpha_1 s_{\max} + p_1 h} + \frac{1}{C_2\alpha_2 s_{\max} + p_2 h}\right),$$

while

$$\mathscr{I}(p_1,p_2) = \max\{|\nu_1(p_1,p_2)|, |\nu_2(p_1,p_2)|\},$$

with

$$\nu_1(p_1,p_2) = p_s\left(\frac{1}{C_2\alpha_2 s_{\max} + p_2 h} - \frac{1}{\alpha_1 s_{\min} + p_1 h}\right)$$

and

$$\nu_2(p_1,p_2) = p_s\left(\frac{1}{C_1\alpha_2 s_{\min} + p_2 h} - \frac{1}{\alpha_1 s_{\max} + p_1 h}\right).$$

Here C_1 *and* C_2 *are positive constants while* $s_{\min}$ *and* $s_{\max}$ *denote the smallest and largest eigenvalues of matrix* S_1 *respectively.*

Proof Following Lemma 3.1 we find upper bounds for $\rho(X+Y)$ and $\rho(X-Y)$. The spectrum of $X+Y$ can be written in terms of the spectra of S_1 and S_2:

$$\sigma(X+Y) = \left\{1 - p_s\left(\frac{1}{\alpha_1 s + p_1 h} + \frac{1}{\alpha_2 t + p_2 h}\right) : s \in \sigma(S_1), t \in \sigma(S_2)\right\}.$$

Let $t_{\min}$ and $t_{\max}$ denote the smallest and largest eigenvalues of S_2 respectively. It is known (see [23] Proposition 4.1.2) that S_1 and S_2 are spectrally equivalent, so there exists positive constants C_1 and C_2 independent of h such that

$$C_1 s_{\min} \leq t_{\min} \qquad \text{and} \qquad t_{\max} \leq C_2 s_{\max}. \tag{3.6}$$

Now (3.6) gives

$$\begin{aligned}\sigma_{\min}(X+Y) &\geq 1 - p_s \max_{\substack{s\in\sigma(S_1)\\ t\in\sigma(S_2)}} \left\{ \frac{1}{\alpha_1 s + p_1 h} + \frac{1}{\alpha_2 t + p_2 h} \right\} \\ &= 1 - p_s \left(\frac{1}{\alpha_1 s_{\min} + p_1 h} + \frac{1}{\alpha_2 t_{\min} + p_2 h} \right) \\ &\geq \underbrace{1 - p_s \left(\frac{1}{\alpha_1 s_{\min} + p_1 h} + \frac{1}{C_1 \alpha_2 s_{\min} + p_2 h} \right)}_{\mu_1(p_1,p_2)}\end{aligned}$$

and

$$\begin{aligned}\sigma_{\max}(X+Y) &\leq 1 - p_s \min_{\substack{s\in\sigma(S_1)\\ t\in\sigma(S_2)}} \left\{ \frac{1}{\alpha_1 s + p_1 h} + \frac{1}{\alpha_2 t + p_2 h} \right\} \\ &= 1 - p_s \left(\frac{1}{\alpha_1 s_{\max} + p_1 h} + \frac{1}{\alpha_2 t_{\max} + p_2 h} \right) \\ &\leq \underbrace{1 - p_s \left(\frac{1}{\alpha_1 s_{\max} + p_1 h} + \frac{1}{C_2 \alpha_2 s_{\max} + p_2 h} \right)}_{\mu_2(p_1,p_2)},\end{aligned}$$

then we have that $\rho(X+Y) \leq \mathscr{R}(p_1,p_2) = \max\{|\mu_1(p_1,p_2)|, |\mu_2(p_1,p_2)|\}$.

The spectrum of $X-Y$ can also be written in terms of the spectra of S_1 and S_2, then similar calculations as above yield that $\rho(X-Y) \leq \mathscr{I}(p_1,p_2)$.

□

As $\mathscr{R}(p_1,p_2)$ and $\mathscr{I}(p_1,p_2)$ are functions of p_1 and p_2, by choosing suitable Robin parameters we hope to make □ "well conditioned" in the sense that GMRES converges quickly. From (3.2) we see that convergence will be quicker if □ is small and far away from the origin. In principle to achieve this we need to minimise both $\mathscr{R}(p_1,p_2)$ and $\mathscr{I}(p_1,p_2)$ however, since □ only approaches the origin along the real axis we choose to focus on minimising $\mathscr{R}(p_1,p_2)$. We are still interested in $\mathscr{I}(p_1,p_2)$ especially to ensure our choice of parameters doesn't cause □ to be too large in the imaginary direction.

4 Optimised Robin parameters

4.1 One sided Robin parameters

Our first choice of Robin parameters is the simplest case when we have the same parameters on both sides of the interface, $p_1 = p_2 = q$. Then we have to minimise $\mathscr{R}^{[1]}(q) = \max\{|\mu_1^{[1]}(q)|, |\mu_2^{[1]}(q)|\}$, where

$$\mu_1^{[1]}(q) = 1 - qh \left(\frac{1}{\alpha_1 s_{\min} + qh} + \frac{1}{C_1 \alpha_2 s_{\min} + qh} \right)$$

and

$$\mu_2^{[1]}(q) = 1 - qh\left(\frac{1}{\alpha_1 s_{\max} + qh} + \frac{1}{C_2\alpha_2 s_{\max} + qh}\right).$$

We also have that $\mathscr{I}^{[1]}(q) = \max\{|v_1^{[1]}(q)|, |v_2^{[1]}(q)|\}$, with

$$v_1^{[1]}(q) = qh\left(\frac{1}{C_2\alpha_2 s_{\max} + qh} - \frac{1}{\alpha_1 s_{\min} + qh}\right)$$

and

$$v_2^{[1]}(q) = qh\left(\frac{1}{C_1\alpha_2 s_{\min} + qh} - \frac{1}{\alpha_1 s_{\max} + qh}\right)$$

This choice of one sided parameter not only simplifies the analysis but guarantees that both $\mathscr{R}^{[1]}(q) < 1$ and $\mathscr{I}^{[1]}(q) < 1$ for all $q > 0$. Then $W(A_{2LM})$ does not contain the origin and (3.2) will hold.

Theorem 4.1 *The unique minimiser, $q^* > 0$, of $\mathscr{R}^{[1]}(q)$ is given by the solution of*

$$\mu_1^{[1]}(q) = -\mu_2^{[1]}(q). \tag{4.1}$$

Proof Taking partial derivatives of $\mu_1^{[1]}(q)$ and $\mu_2^{[1]}(q)$ with respect to q we have that

$$\frac{\partial \mu_1^{[1]}}{\partial q} < 0 \qquad \text{and} \qquad \frac{\partial \mu_2^{[1]}}{\partial q} < 0,$$

for all $q > 0$. Moreover $\mu_j^{[1]}(0) = 1$ and $\lim_{q\to\infty} \mu_j^{[1]}(q) = -1$ for $j = 1, 2$. Then since $\mu_j^{[1]}(q)$ is a monotonically decreasing, continuous function $|\mu_j^{[1]}(q)|$ reaches its minimum when $\mu_j^{[1]}(q) = 0$. Solving $\mu_j^{[1]}(q) = 0$ for q we find that $|\mu_1^{[1]}(q)|$ reaches its minimum at

$$q_1 = \frac{\sqrt{C_1\alpha_1\alpha_2}s_{\min}}{h},$$

while $|\mu_2^{[1]}(q)|$ reaches its minimum at

$$q_2 = \frac{\sqrt{C_2\alpha_1\alpha_2}s_{\max}}{h}.$$

It follows that the minimiser q^* of $\mathscr{R}^{[1]}(q)$ must lie in the interval $[q_1, q_2]$. To see this, note that when $q < q_1$ increasing q uniformly decreases both $|\mu_1^{[1]}(q)|$ and $|\mu_2^{[1]}(q)|$. On the other hand if $q > q_2$ decreasing q uniformly decreases both $|\mu_1^{[1]}(q)|$ and $|\mu_2^{[1]}(q)|$, see Figure 4.1.

Now in the interval $[q_1, q_2]$, $|\mu_1^{[1]}(q)|$ is monotonically increasing and $\mu_2^{[1]}(q)$ is monotonically decreasing, so $\mathscr{R}^{[1]}(q)$ must reach its minimum when

$$|\mu_1^{[1]}(q)| = |\mu_2^{[1]}(q)|.$$

That is when

$$\mu_1^{[1]}(q) = -\mu_2^{[1]}(q).$$

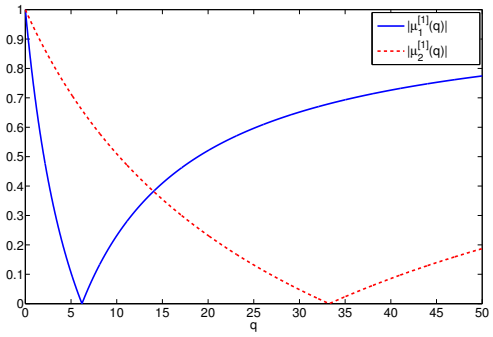

Fig. 4.1 upper bound $\mathscr{R}^{[1]}(q)$ for different values of the one sided Robin parameter q

□

Calculating the minimising Robin parameter in (4.1) involves solving a quartic equation. To simplify the convergence analysis we propose to choose an approximation to q^* by taking the geometric mean of the endpoints of the interval $[q_1, q_2]$. Then we obtain the one sided Robin parameter:

$$\hat{q} = \frac{\sqrt{\sqrt{C_1 C_2}\alpha_1 \alpha_2 s_{\min} s_{\max}}}{h}. \tag{4.2}$$

Let $\square_{\hat{q}}$ denote the rectangle defined by $\mathscr{R}^{[1]}(\hat{q})$ and $\mathscr{I}^{[1]}(\hat{q})$. To approximate the convergence speed of GMRES with this choice of Robin parameter we must construct the conformal map, from the exterior of $\square_{\hat{q}}$ to the interior of the unit disc. We cannot state such a map explicitly but can define its inverse.

Lemma 4.1 *Let $\Psi : w \mapsto z$ denote the conformal map from the interior of the unit disc to the exterior of $\square_{\hat{q}}$, with $\Psi(0) = \infty$. Furthermore let $\delta \in (0, 1/2)$ denote the distance, measured along the real axis, from the origin to left hand boundary of $\square_{\hat{q}}$. Then Ψ is of the form:*

$$\Psi(w, \delta) = \delta + C(\psi(w, \theta) - \psi(1, \theta)), \tag{4.3}$$

where

$$\psi(w, \theta) = \int^w \zeta^{-2} \left((1 - e^{i\theta}\zeta)(1 - e^{-i\theta}\zeta)(1 + e^{i\theta}\zeta)(1 + e^{-i\theta}\zeta) \right)^{1/2} d\zeta. \tag{4.4}$$

Here $\theta \in (0, \pi/2)$ determines the aspect ratio and $C \in \mathbb{R}^+$ the scaling of $\square_{\hat{q}}$.

Proof Let $\Xi(w)$ denote the conformal map from the interior of the unit disc to the exterior of an arbitrary rectangle. A *Schwarz-Christoffel mapping* can be used to construct such a map of the form:

$$\Xi(w) = A + C \int^w \zeta^{-2} \prod_{k=1}^{4} \left(1 - \frac{\zeta}{w_k} \right)^{1/2} d\zeta,$$

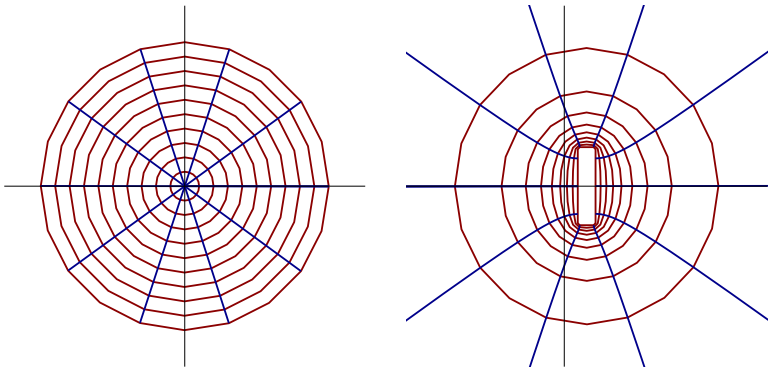

Fig. 4.2 conformal mapping from the interior of the unit disc to the exterior of $\square_{\hat{q}}$

where complex constants A and C correspond to translation and scaling/rotation of the rectangle respectively. The w_k's in the integrand are pre-vertices, where $\Xi(w_k) = z_k$, chosen on the boundary of the unit disc to determine the side lengths of the rectangle. For full details of Schwarz-Christoffel mappings see [4].

Rectangle $\square_{\hat{q}}$ is situated in the right-half plane, centred at the point $(1/2,0)$ and with sides parallel to the imaginary axis. For a given angle $\theta \in (0,\pi/2)$ consider the choice of pre-vertices $w_1 = e^{-i\theta}$, $w_2 = e^{i\theta}$, $w_3 = -e^{-i\theta}$ and $w_4 = -e^{i\theta}$. Then (4.4) gives the map from the interior of the unit disc to the exterior of the rectangle centred at the origin with sides parallel to the imaginary axis. The choice of θ will determine the aspect ratio of the rectangle, with $\theta = 0$ giving an interval of the real axis, $\theta = \pi/4$ a square and $\theta = \pi/2$ an interval of the imaginary axis.

Now consider the mapping

$$\Psi(w) = A + C\psi(w,\theta). \tag{4.5}$$

Then, for suitably chosen A, C and θ, (4.5) gives the map to the exterior of $\square_{\hat{q}}$, where we need only take A and C to be real and positive.

To this end we can eliminate one of the three unknowns by observing that mapping (4.4) takes the point $w = 1$ on the boundary of the unit disc to the left hand boundary point, on the real axis, of the rectangle. We know, for $\square_{\hat{q}}$, that the distance of this point from the origin is given by $\delta = \frac{1}{2} - \frac{1}{2}\mathscr{R}^{[1]}(\hat{q})$ and so

$$\delta = A + C\psi(1,\theta).$$

Solving the above for A and substituting into (4.5) we recover the conformal map (4.3) to the exterior of $\square_{\hat{q}}$, as shown in Figure 4.2.

□

We are interested in the convergence speed of GMRES when h becomes small, i.e. the finite element mesh size becomes finer, and when the jump in diffusion coefficients α_1 and α_2 becomes large.

Theorem 4.2 *Let the 2LM method system (1.3), with choice of Robin parameter (4.2), be solved using GMRES. Assume that α_1 and α_2 are held constant. Let $s_{\max} =$*

C_3/h and $h \to 0$. The estimated asymptotic convergence factor of GMRES for small h is

$$\rho = 1 - O(\sqrt{h}). \tag{4.6}$$

Assume that α_1 and h are held constant and let $\alpha_2 \to 0$. The estimated asymptotic convergence factor of GMRES for small α_2 is

$$\rho = \beta + O(\sqrt{\alpha_2}), \tag{4.7}$$

where β is a constant, with $\beta < 1$.

Proof Let $\Phi(z,\delta)$ denote the conformal map from the exterior of $\square_{\hat{q}}$ to the interior of the unit disc. Then (4.3) gives the inverse of $\Phi(z,\delta)$. Taking the linear approximation of $\Psi(w,\delta)$ near $w = 1$, denoted $\overline{\Psi}(w,\delta)$, we obtain

$$\overline{\Psi}(w,\delta) = \delta + \frac{c_1}{c_2} C(w-1),$$

where

$$c_1 = 8\cos^2\theta\cos 2\theta + 8\sin\theta\cos t\sin 2\theta - \sin 4\theta\sqrt{2-2\cos 4\theta} - 7\cos 2\theta - \cos 6\theta$$

and

$$c_2 = \sqrt{2-2\cos 2\theta}(1+\cos 4\theta + \sin 2\theta\sqrt{2-2\cos 4\theta}).$$

Solving $\overline{\Psi}(w,\delta) = 0$ for w gives the linear approximation of the mapping from the origin, exterior to $\square_{\hat{q}}$, to the interior of the unit disc:

$$\overline{\Phi}(0,\delta) = 1 - \frac{c_2}{c_1}\frac{\delta}{C}. \tag{4.8}$$

Then from (3.2) we have that the estimated asymptotic convergence factor of GMRES is $\rho = \overline{\Phi}(0,\delta)$, where we have dropped the absolute value since, for suitable C and θ, $\overline{\Phi}(0,\delta)$ is real and positive.

When either h or α_2 is small $|\mu_1^{[1]}(\hat{q})| > |\mu_2^{[1]}(\hat{q})|$ and $\mu_1^{[1]}(\hat{q}) < 0$, then we have that

$$\delta = \frac{1}{2} + \frac{1}{2}\mu_1^{[1]}(\hat{q}). \tag{4.9}$$

Substituting (4.9) into (4.8) and taking the series expansion as α_2 goes to zero gives the second result:

$$\begin{aligned}\rho &= \beta \\ &+ \frac{1}{2}\frac{(\sqrt{C_1C_2}s_{\max} - C_1 s_{\min})\sqrt{2-2\cos 4\theta}(1+\cos 4\theta + \sin 2\theta\sqrt{2-2\cos 4\theta})}{\sqrt{\sqrt{C_1C_2}\alpha_1 s_{\min}s_{\max}}C(4-3\cos 2\theta - \sin 4\theta\sqrt{2-2\cos 4\theta} - \cos 6\theta))}\sqrt{\alpha_2} \\ &+ O(\alpha_2),\end{aligned}$$

where

$$\begin{aligned}\beta = \frac{1}{2}&\frac{\sqrt{2-2\cos 4\theta}(2C\sin 4\theta + \sin 2\theta\sqrt{2-2\cos 2\theta})}{C(\cos 6\theta + \sin 4\theta\sqrt{2-2\cos 4\theta} + 3\cos 2\theta - 4)} \\ &+ \frac{1}{2}\frac{\sqrt{2-2\cos 2\theta}(1+\cos 4\theta) + C(6\cos 2\theta + 2\cos 6\theta - 8)}{C(\cos 6\theta + \sin 4\theta\sqrt{2-2\cos 4\theta} + 3\cos 2\theta - 4)},\end{aligned}$$

with $\beta < 1$.

It is known, [1], for small h that there exists constant C_3, independent of h, such that $s_{\max} = C_3/h$. Substituting this and (4.9) into (4.8) and taking the series expansion as h goes to zero gives the first result:

$$\begin{aligned}\rho =& 1 \\ & - \frac{1}{2}\frac{(\alpha_1 + C_1\alpha_2)\sqrt{s_{\min}}\sqrt{2-2\cos 2\theta}(1+\cos 4\theta + \sin 2\theta\sqrt{2-2\cos 4\theta})}{\sqrt{\sqrt{C_1C_2}C_3\alpha_1\alpha_2}C(4-3\cos 2\theta - \sin 4\theta\sqrt{2-2\cos 4\theta} - \cos 6\theta)}\sqrt{h} \\ & + O(h)\end{aligned}$$

□

Remark 4.1 The convergence shown in (4.6) for small h is an improvement on the other popular estimate for GMRES (see [27] Lemma C.11) that gives an asymptotic convergence factor of $1 - O(h)$ when solving the 2LM method system.

Estimate (4.7) shows that the larger the jump in the diffusion coefficients the faster GMRES will converge. This is an improvement from other popular DDMs such as FETI-DP and Neumann-Neumann that are independent of jumps in the coefficients, [21].

4.2 Scaled one sided Robin parameters

A second choice of parameters is again to minimise only one parameter but to now take into account the jump in coefficients across the interface. It was shown in [6,7, 20] for the OSM that the choice $p_1 = \alpha_2 r$ and $p_2 = \alpha_1 r$ leads to faster convergence as the jump in coefficients becomes larger. In the literature these are referred to as scaled one sided or one and a half Robin parameters. The downside to choosing $p_1 \neq p_2$ is that for some values of r the field of values of A_{2LM} may contain the origin and so (3.2) will not hold.

We need to minimise $\mathscr{R}^{[1.5]}(r) = \max\{|\mu_1^{[1.5]}(r)|, |\mu_2^{[1.5]}(r)|\}$, where

$$\mu_1^{[1.5]}(r) = 1 - \frac{(\alpha_1+\alpha_2)rh}{2}\left(\frac{1}{\alpha_1 s_{\min} + \alpha_2 rh} + \frac{1}{C_1\alpha_2 s_{\min} + \alpha_1 rh}\right)$$

and

$$\mu_2^{[1.5]}(r) = 1 - \frac{(\alpha_1+\alpha_2)rh}{2}\left(\frac{1}{\alpha_1 s_{\max} + \alpha_2 rh} + \frac{1}{C_2\alpha_2 s_{\max} + \alpha_1 rh}\right).$$

Theorem 4.3 *The unique minimiser, $r^* > 0$, of $\mathscr{R}^{[1.5]}(r)$ is given by the solution of*

$$\mu_1^{[1.5]}(r) = -\mu_2^{[1.5]}(r). \tag{4.10}$$

Proof We proceed in a similar fashion as we did for Theorem 4.1. Taking the partial derivatives of $\mu_1^{[1.5]}(r)$ and $\mu_2^{[1.5]}(r)$ with respect to r we see that

$$\frac{\partial \mu_1^{[1.5]}}{\partial r} < 0 \qquad \text{and} \qquad \frac{\partial \mu_2^{[1.5]}}{\partial r} < 0,$$

for all $r > 0$. Moreover $\mu_j^{[1.5]}(0) = 1$ and $\lim_{r\to\infty} \mu_j^{[1.5]}(r) = -\frac{1}{2}\frac{\alpha_1^2+\alpha_2^2}{\alpha_1\alpha_2}$, for $j = 1, 2$. Let

$$D_j = \alpha_1^4 + (6C_j - 2)\alpha_1^3\alpha_2 + (C_j^2 + 4C_j + 1)\alpha_1^2\alpha_2^2 + (6C_j - 2C_j^2)\alpha_1\alpha_2^2 + C_j\alpha_2^4,$$

then $|\mu_1^{[1.5]}(r)|$ reaches its minimum at

$$r_1 = \frac{\left(\alpha_1^4 - (C_1+1)\alpha_1\alpha_2 + C_1\alpha_2^2 + \sqrt{D_1}\right) s_{\min}}{2(\alpha_1^2+\alpha_2^2)h}$$

and $|\mu_2^{[1.5]}(r)|$ reaches its minimum at

$$r_2 = \frac{\left(\alpha_1^4 - (C_2+1)\alpha_1\alpha_2 + C_2\alpha_2^2 + \sqrt{D_2}\right) s_{\max}}{2(\alpha_1^2+\alpha_2^2)h}.$$

It follows that since $\mu_1^{[1.5]}(r)$ and $\mu_2^{[1.5]}(r)$ are monotonically decreasing functions the minimiser r^* must lie in the interval $[r_1, r_2]$.

Then we have that in the interval $[r_1, r_2]$, $|\mu_1^{[1.5]}(r)|$ is monotonically increasing and $|\mu_2^{[1.5]}(r)|$ is monotonically decreasing. So the unique minimiser r^* is obtained when

$$|\mu_1^{[1.5]}(r)| = |\mu_2^{[1.5]}(r)|.$$

That is when

$$\mu_1^{[1.5]}(r) = -\mu_2^{[1.5]}(r).$$

□

Remark 4.2 The minimising scaled one sided Robin parameter r^* results in $W(A_{2LM})$ containing the origin, so we cannot derive a convergence estimate of the form (3.2). However we will see in the numerical experiments in the next section that this choice of parameters leads to faster convergence as compared to the non-scaled one sided case.

Remark 4.3 It is also possible to take p_1 and p_2 to be two independent parameters on each side of the interface. It was shown for the OSM in symmetric rectangular subdomains, [6], that this choice leads to even faster convergence than either one sided or scaled one sided Robin parameters. However for general subdomains these so called two sided parameters are difficult to derive.

5 Numerical experiments

We consider model problem (1.1) on the L-shaped domain $\Omega \subset \mathbb{R}^2$, which is partitioned into nonoverlapping subdomains as shown in Figure 5.1. The diffusion coefficient is given by

$$a(x,y) = \begin{cases} \alpha_1(1 + \frac{1}{2}\sin(3\pi x)\cos(3\pi y)) & \text{in} \quad \Omega_1 \\ \alpha_2(1 + \frac{1}{2}\sin(3\pi x)\cos(3\pi y)) & \text{in} \quad \Omega_2 \end{cases}$$

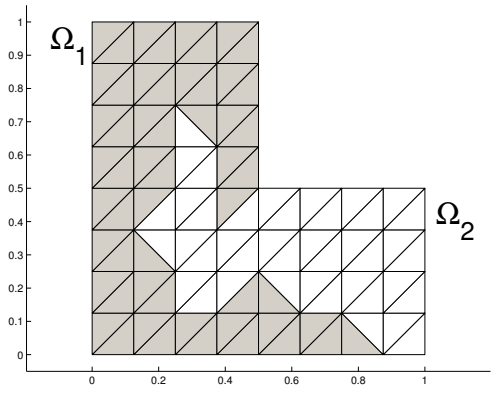

Fig. 5.1 nonoverlapping decomposition of an L-shaped domain into two general subdomains

and the forcing term by

$$f(x,y) = 1 + \alpha_1 \alpha_2 \sin(3\pi x) \sin(3\pi y).$$

We perform a uniform triangulation of Ω, with mesh parameter h, and discretise the PDE using piecewise linear, triangular finite elements. Let $\omega = \alpha_1/\alpha_2$, such that $\alpha_1 > \alpha_2$. We set $\alpha_1 = 1$ and let α_2 vary. We solve system (1.3) using the built in GMRES solver in MATLAB for different choices of h and ω. We use GMRES without restarts, a zero vector initial guess and are interested in the number of iterations required to reach a tolerance of 10^{-12} in the relative residual. We also calculate the 2-norm condition number of A_{2LM} using the MATLAB command `cond`.

Note that our choice of one sided parameters given in (4.2) involves constants C_1 and C_2 that, in general, we do not know. Then we choose to set $C_1 = C_2 = 1$, which corresponds to the case of symmetric subdomains about the interface. We do not have symmetric subdomains for our example, but as we will see even with this simplification we can still achieve fast convergence. Then the one sided Robin parameter we use is

$$\tilde{q} = \frac{\sqrt{a_1 a_2 s_{\min} s_{\max}}}{h}. \tag{5.1}$$

Eigenvalues $s_{\min}$ and $s_{\max}$ are calculated in MATLAB using the `eig` command. For larger problems where this approach would be impractical, due to S_1 and S_2 being dense, the estimates $s_{\min} = b_1$ and $s_{\max} = b_2/h$, for constants b_1 and b_2, (see [1]) can be used. The results for the one sided Robin parameter are shown in Table 5.1 for different values of h and ω.

The numerical results confirm our theoretical results from Theorem 4.2. Decreasing the mesh size h requires more iterations of GMRES will increasing the jump in coefficients requires less. Though in general the condition number of a nonsymmetric matrix is not useful in determining the speed of convergence of GMRES here we see favourable behaviour of the condition number of A_{2LM} with one sided parameters.

	$h = 1/16$	$h = 1/32$	$h = 1/64$	$h = 1/128$
$\omega = 10^1$	**26** (2.7768)	**31** (3.8800)	**37** (5.4121)	**43** (7.5992)
$\omega = 10^2$	**22** (1.6023)	**24** (1.9519)	**27** (2.4270)	**32** (3.0963)
$\omega = 10^3$	**16** (1.1882)	**18** (1.2909)	**20** (1.4280)	**22** (1.6196)
$\omega = 10^4$	**13** (1.0590)	**14** (1.0903)	**14** (1.1314)	**16** (1.1880)
$\omega = 10^5$	**10** (1.0186)	**12** (1.0283)	**12** (1.0411)	**12** (1.0585)

Table 5.1 number of iterations of GMRES (in bold) and the condition number of A_{2LM} matrix (in brackets) using one sided Robin parameter (5.1)

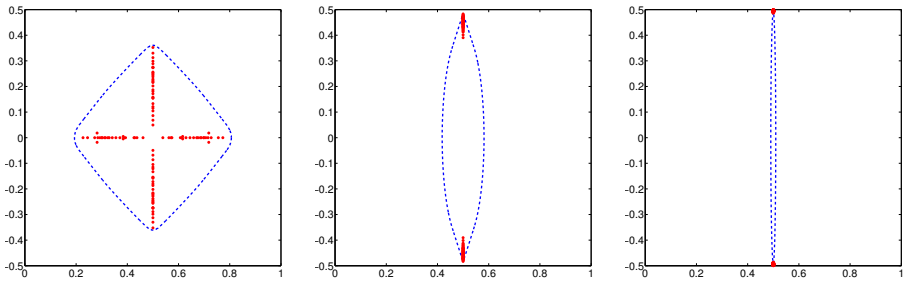

Fig. 5.2 $W(A_{2LM})$ (dashed line) and $\sigma(A_{2LM})$ (dots) with choice of one sided Robin parameter (5.1), $h = 1/32$, $\omega = 10^1$ on left, $\omega = 10^3$in middle and $\omega = 10^5$ on right

In Figure 5.2 we plot the spectrum and field of values of A_{2LM} for different values of ω with one sided parameters. We see that as the jump in coefficients becomes larger the field of values moves further away from the origin while the eigenvalues become more clustered together and are pure imaginary, resulting in the faster convergence of GMRES.

For the case of scaled one sided parameters as in the case of one sided parameters the minimising parameter from (4.10) involves the solution of a quartic equation. So we choose to approximate the parameter by taking the geometric mean of the endpoints of the interval $[r_1, r_2]$, as defined in Theorem 4.3, in which r^* lies. Again we set $C_1 = C_2 = 1$, then the scaled one sided Robin parameter we use is given by

$$\tilde{r} = \frac{\sqrt{s_{\min} s_{\max}}}{h}. \tag{5.2}$$

The results for this choice for different values of h and ω are shown in Table 5.2 while the spectrum and field of values of A_{2LM} for different values of ω are shown in Figure 5.3.

For scaled one sided parameters we observe similar behaviour as we do for the non-scaled parameters. The number of iterations increases as we decrease h and decreases as we increase ω. However, the number of iterations needed to reach the

same tolerance is significantly less. For small h and large ω we require about half the number of iterations as are required for the non-scaled case. Figure 5.3 goes some way to explain this as we see that as ω increases the eigenvalues of A_{2LM} become clustered about the point $(1/2,0)$, whereas in the non-scaled case the clustering happens around two points. GMRES can more easily deal with systems whose matrix's eigenvalues are clustered together away from the origin and are on the real line.

We also observe from Figure 5.3 that as ω increases the size of $W(A_{2LM})$ increases and that the boundary of $W(A_{2LM})$ moves further away from the set of eigenvalues. This is due to the high non-normality of matrix A_{2LM} when we have scaled one sided parameters. The field of values is a good approximation of the spectrum of a matrix when said matrix is not too highly non-normal, [8], as is the case when we have non-scaled one sided parameters. Despite this, as we see from Table 5.2 the approach of minimising $W(A_{2LM})$ for scaled one sided parameters results in much faster convergence of GMRES.

	$h = 1/16$	$h = 1/32$	$h = 1/64$	$h = 1/128$
$\omega = 10^1$	**19** (7.5443)	**22** (14.0651)	**26** (25.2644)	**29** (43.6511)
$\omega = 10^2$	**12** (13.2178)	**13** (28.5038)	**14** (60.1054)	**15** (123.3700)
$\omega = 10^3$	**8** (14.3136)	**9** (31.4972)	**10** (68.1422)	**10** (144.5996)
$\omega = 10^4$	**6** (14.4360)	**6** (31.8268)	**8** (69.0434)	**8** (147.0497)
$\omega = 10^5$	**6** (14.4480)	**6** (31.8601)	**6** (69.1346)	**6** (147.2984)

Table 5.2 number of iterations of GMRES (in bold) and the condition number of A_{2LM} matrix (in brackets) using scaled one sided Robin parameter (5.2)

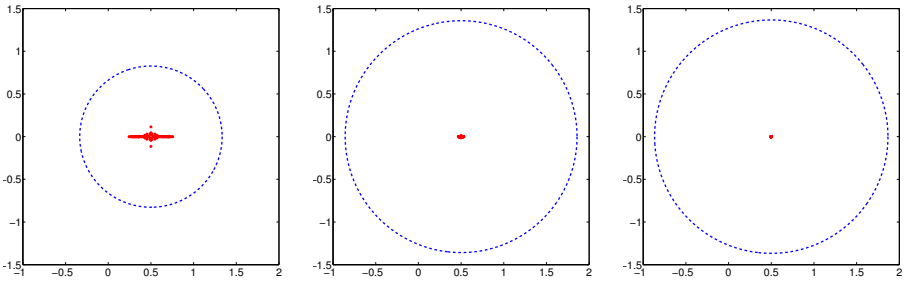

Fig. 5.3 $W(A_{2LM})$ (dashed line) and $\sigma(A_{2LM})$ (dots) with choice of scaled one sided Robin parameter (5.2), $h = 1/32$, $\omega = 10^1$ on left, $\omega = 10^3$ in middle and $\omega = 10^5$ on right

References

1. Brenner, S.C.: The condition number of the schur complement in domain decomposition. Numer. Math. **83**(2), 187–203 (1999)
2. Deng, Q.: Timely communicaton: An analysis for a nonoverlapping domain decomposition iterative procedure. SIAM J. Sci. Comput. **18**(5), 1517–1525 (1997)
3. Driscoll, T.A., Toh, K.C., Trefethen, L.N.: From potential theory to matrix iterations in six steps. SIAM Rev. **40**(3), 547–578 (1998)
4. Driscoll, T.A., Trefethen, L.N.: Schwarz-Christoffel Mapping. Cambridge University Press (2002)
5. Drury, S.W., Loisel, S.: Sharp condition number estimates for the symmetric 2-lagrange multiplier method. In: Domain Decomposition Methods in Science and Engineering XX, pp. 255–261. Springer (2013)
6. Dubois, O.: Optimized schwarz methods for the advection-diffusion equation and for problems with discontinuous coefficients. Ph.D. thesis, McGill University (2007)
7. Dubois, O., Lui, S.: Convergence estimates for an optimized schwarz method for PDEs with discontinuous coefficients. Numer. Algorithms **51**(1), 115–131 (2009)
8. Embree, M.: How descriptive are GMRES convergence bounds? Tech. rep., Oxford University Computing Laboratory (1999)
9. Farhat, C., Macedo, A., Lesoinne, M., Roux, F.X., Magoulés, F., De La Bourdonnaie, A.: Two-level domain decomposition methods with lagrange multipliers for the fast iterative solution of acoustic scattering problems. Comput. Methods in Appl. Mech. Eng. **184**(2), 213–239 (2000)
10. Gander, M.J.: Optimized schwarz methods. SIAM J. Numer. Anal. **44**(2), 699–731 (2006)
11. Gander, M.J., Halpern, L., Nataf, F.: Optimized schwarz methods. In: Twelth International Conference on Domain Decomposition Methods, pp. 15–28. Domain Decomposition Press, Bergen (2001)
12. Gander, M.J., Kwok, F.: Best robin parameters for optimized schwarz methods at cross points. SIAM J. Sci. Comput. **34**(4), A1849–A1879 (2012)
13. Gander, M.J., Magoules, F., Nataf, F.: Optimized schwarz methods without overlap for the helmholtz equation. SIAM J. Sci. Comput. **24**(1), 38–60 (2002)
14. Gander, M.J., et al.: Schwarz methods over the course of time. Electron. Trans. Numer. Anal. **31**(5), 228–255 (2008)
15. Horn, R.A., Johnson, C.R.: Topics in matrix analysis. Cambridge University Press (1991)
16. Johnson, C.R.: Numerical determination of the field of values of a general complex matrix. SIAM J. Numer. Anal. **15**(3), 595–602 (1978)
17. Lions, P.L.: On the schwarz alternating method. iii: a variant for nonoverlapping subdomains. In: Third international symposium on domain decomposition methods for partial differential equations, vol. 6, pp. 202–223. SIAM, Philadelphia, PA (1990)
18. Loisel, S.: Condition number estimates for the nonoverlapping optimized schwarz method and the 2-lagrange multiplier method for general domains and cross points. SIAM J. Numer. Anal. **51**(6), 3062–3083 (2013)
19. Lui, S.: A lions non-overlapping domain decomposition method for domains with an arbitrary interface. IMA J. Numer. Anal. **29**(2), 332–349 (2009)
20. Maday, Y., Magoulès, F.: Optimized schwarz methods without overlap for highly heterogeneous media. Comput. Methods in Appl. Mech. Eng. **196**(8), 1541–1553 (2007)
21. Mathew, T.P.A.: Domain decomposition methods for the numerical solution of partial differential equations. Springer (2008)
22. Nevanlinna, O.: Convergence of interations for linear equations. Springer (1993)
23. Quarteroni, A., Valli, A., et al.: Domain decomposition methods for partial differential equations. Oxford University Press (1999)
24. Roux, F.X., Magoulès, F., Salmon, S., Series, L.: Optimization of interface operator based on algebraic approach. In: Fourteenth International Conference on Domain Decomposition Methods, pp. 297–304. Domain Decomposition Press, Bergen (2003)
25. Saad, Y., Schultz, M.H.: GMRES: A generalized minimal residual algorithm for solving nonsymmetric linear systems. SIAM J. Sci. Stat. Comput **7**(3), 856–869 (1986)
26. Schwarz, H.A.: Über einen grenzübergang durch altermierendes verfahren. Vierteljahrsschrift der Naturforschenden Gesellschaft in Zürich **15**, 272–286 (1870)
27. Toselli, A., Widlund, O.: Domain decomposition methods: algorithms and theory. Springer (2005)